Time-Dependent Disruption of Oviduct Pacemaker Cells by *Chlamydia* Infection in Mice[1]

Rose Ellen Dixon,[3] **Kyle H. Ramsey,**[4] **Justin H. Schripsema,**[4] **Kenton M. Sanders,**[3] **and Sean M. Ward**[2,3]

Department of Physiology and Cell Biology,[3] *University of Nevada School of Medicine, Reno, Nevada*
Department of Microbiology and Immunology,[4] *Chicago College of Osteopathic Medicine, Midwestern University,*
Downers Grove, Illinois

ABSTRACT

Chlamydia trachomatis **is the most commonly reported infectious disease in the United States. In women, this infection can lead to pelvic inflammatory disease and cause ectopic pregnancy and tubal factor infertility. Oviduct interstitial cells of Cajal (ICC-OVI) have been identified as pacemakers, responsible for generating slow waves that underlie myosalpinx contractions that are critical for egg transport. ICC-OVI are damaged in mice by the host inflammatory response to** *Chlamydia,* **leading to loss of pacemaker activity and associated contractions. However the inflammatory mediator(s) that causes this damage has not been identified. Mice resolve** *C. muridarum* **3–4 wk postinfection but it remains unexplored whether ICC-OVI and pacemaker activity recovers. We have investigated the time dependence of** *C. muridarum* **infection with respect to ICC-OVI loss and examined the inflammatory mediator(s) that may be responsible for this damage. Intracellular recordings from the myosalpinx were made at 1, 2, 4 and 7 wk postinfection with** *Chlamydia.* **Immunohistochemistry was performed at similar time points to examine changes in ICC-OVI networks and expression of nitric oxide synthase 2 (NOS2) and prostaglandin synthase 2 (PTGS2).** *Chlamydia*-**induced expression of NOS2 occurred in stellate-shaped, macrophage-like cells, and damage to ICC-OVI and pacemaker activity occurred as NOS2 expression increased. Immunohistochemistry revealed that macrophages were in close proximity to ICC-OVI. Changes to ICC-OVI were not correlated with PTGS2 expression. These data suggest that ICC-OVI networks and pacemaker activity may be damaged by nitric oxide produced in NOS2-expressing macrophages in response to** *C. muridarum* **infection. As the infection resolves, NOS2 expression decreases, ICC-OVI networks recover, and pacemaker activity resumes.**

Chlamydia, *fallopian tubes, female reproductive tract, interstitial cells of Cajal, NOS2, oviduct, smooth muscle*

INTRODUCTION

Chlamydia trachomatis is the most commonly reported infectious disease in the United States [1]. More than 1 million

new cases of *C. trachomatis* infection were reported to the Centers for Disease Control and Prevention in 2008, representing a 9.2% increase in cases from the previous year. *Chlamydia* infections are asymptomatic in 70%–75% of women and as a consequence often go undiagnosed, untreated, and unreported [2]. Almost three times more women are diagnosed with *Chlamydia* than men [1]. Serious health consequences of *Chlamydia* infections are more common in females and, if left untreated, can lead to pelvic inflammatory disease (PID), which can result in chronic pelvic pain, in increased risk of ectopic pregnancy, and ultimately in tubal factor infertility [1]. Postinfection damage to the Fallopian tubes is estimated to be responsible for 30%–40% of female infertility [3].

A murine strain of *Chlamydia, C. muridarum,* has provided an animal model of *Chlamydia* to investigate the host immune response to infection [4]. Intravaginal inoculation of susceptible strains of mice with *C. muridarum* produces an ascending infection that is reminiscent of human *Chlamydia* infection and has similar sequelae, including salpingitis (inflammation of the oviducts), pyosalpinx (pus-filled oviduct, indicative of salpingitis), hydrosalpinx (fluid-filled oviduct that occurs secondary to salpingitis), and infertility [5, 6]. The genetic profile of *C. muridarum* is similar to that of human *C. trachomatis* serovar D, and it appears to be accepted that *C. muridarum* infection provides a reasonable approximation of the acute phase of infection seen in humans [4, 7, 8].

Smooth muscle of the oviduct (myosalpinx) is driven by spontaneous electrical slow waves that depolarize the cells and initiate phasic contractions. These contractions of the myosalpinx are vital for egg transport along the duct [9]. Slow waves have been recorded from oviducts of several species, including mice [9, 10], guinea pigs [10, 11], baboons [10], and humans [12]. We recently showed in mice that slow waves originate in a population of specialized pacemaker cells, termed oviduct interstitial cells of Cajal (ICC-OVI), as identified by KIT-like immunoreactivity [9]. Similar cells have been identified in Fallopian tubes of humans, where they are referred to as tubal-ICC or interstitial cell of Cajal-like cells. Based on morphology, others have also postulated a role for these cells as pacemakers in humans [13–15].

Infection of mice with *C. muridarum* induces a host inflammatory response that damages ICC-OVI and pacemaker activity, rendering oviducts quiescent electrically and unable to generate propulsive contractions [9]. The host immune response that damaged ICC-OVI was proposed to involve induction of nitric oxide synthase 2 (NOS2 or inducible nitric oxide synthase) and production of nitric oxide (NO). NOS2 protein was upregulated in infected oviducts in comparison to age-matched controls and oviduct pacemaker activity was rescued by treatment with the NOS2 inhibitor N-([3-(amino-methyl)phenyl]methyl)ethanimidamide (1400W). Because

ICC-OVI are responsible for the generation of slow wave activity that underlies the propulsive contractions of oviducts, we hypothesized that damage to ICC-OVI, resulting from *Chlamydia* infection, leads to oviduct stasis, luminal obstruction, and ultimately infertility if these conditions are not resolved. However, the correlation between onset of the host inflammatory response to *Chlamydia* infection and damage to ICC-OVI has not been investigated.

In the present study we examined the time course of *C. muridarum* infection from onset to resolution with respect to ICC-OVI damage. Our aims were to determine 1) the time dependence of ICC-OVI damage following intravaginal inoculation with *C. muridarum*; 2) whether damage to ICC-OVI was correlated with the upregulation of the inflammatory mediators, NOS2 or prostaglandin synthase 2 (PTGS2, also known as cyclooxygenase-II or COXII) and 3) whether ICC-OVI populations and associated pacemaker activity recover as the *Chlamydia* infection resolves.

MATERIALS AND METHODS

Animal Treatment

BALB/c mice were purchased from Jackson Laboratory (Bar Harbor, ME) or Harlan Sprague-Dawley (Indianapolis, IN). Animals between the ages of 8 and 15 wk were anesthetized by isoflurane (Baxter, Deerfield, IL) inhalation prior to cervical dislocation. The oviducts and uterine horns were removed by sharp dissection and were immediately placed in Krebs Ringer bicarbonate solution (KRB). Oviducts were uncoiled and electrical recordings were made on intact preparations. Maintenance of animals and experiments were performed in accordance with the National Institutes of Health Guide for the Care and Use of Laboratory Animals. All procedures were approved by the Institutional Animal Use and Care Committees at the University of Nevada and Midwestern University.

Electrophysiological Experiments

Electrical activity of the myosalpinx was recorded using intracellular microelectrodes as previously described [9]. In brief, smooth muscle cells within the myosalpinx were impaled using sharp glass microelectrodes with resistances of 80–120 MΩ, inserted into intact oviduct preparations through the serosal layer. In the present study all recordings were made from the isthmus region located approximately 50% along the length of the oviducts. To stabilize the smooth muscle and permit maintenance of intracellular recordings, oviducts were pinned to a Sylgard elastomer (Dow Corning, Midland, MI)-lined recording chamber using 0.127 mm diameter tungsten pins.

Potential differences across cell membranes were recorded using a high-impedance electrometer (Axoclamp 2B; Axon Instruments/Molecular Devices, Sunnyvale, CA), digitized using a Digidata 1322A system, and recorded onto a PC running Axoscope 9.2 (Axon Instruments).

In those oviducts that lacked spontaneous slow wave activity, muscle viability was tested by subjecting preparations to single pulses of electric field stimulation (EFS; 1–10 ms duration) generated by a square wave pulse generator (Grass S48; Grass Medical Instruments, Quincy, MA) and delivered to the tissue via parallel platinum electrodes positioned on either side of the oviduct.

Immunohistochemical Experiments

Oviducts were fixed using acetone (10 min at 4°C) or paraformaldehyde (PFS; 4% w/v in 0.1 M PBS for 30 min at 4°C) and subsequently washed from fixative for 1 h (acetone-fixed) or overnight (PFS-fixed) with multiple changes of PBS (0.01 M, pH 7.2). Tissues were then blocked for 1 h at room temperature with bovine serum albumin (1% w/v; Sigma-Aldrich, St. Louis, MO) before being placed in primary antibody for 48 h at 4°C.

To identify ICC-OVI, rat anti-mouse KIT monoclonal (ACK2, 5 μg ml^{-1}; eBioscience Inc., San Diego, CA [16, 17]) or goat anti-mouse stem cell factor receptor monoclonal (2 μg ml^{-1}; R&D Systems Inc., Minneapolis, MN) antibodies were used. Cells expressing NOS2 and PTGS2 were identified with a rabbit anti-mouse NOS2 polyclonal (5 μg ml^{-1}; BD Biosciences, San Jose, CA) and a rabbit anti-mouse PTGS2 polyclonal (5 μg ml^{-1}; Enzo Life Sciences International, Inc., Plymouth Meeting, PA) respectively. Macrophages were identified with a rat anti-mouse I-A^d/I-E^d monoclonal (10 μg ml^{-1}; Pharmingen, San Diego, CA).

Following primary antibody, tissues were washed with PBS (0.01 M, pH 7.2) followed by incubation in the appropriate Alexa Fluor secondary antibody (Molecular Probes, Eugene, OR; 1:500 in PBS, 1 h at room temperature) before mounting on glass slides with Aqua-Mount (Lerner Laboratories, Pittsburgh, PA). For double labeling, the second primary and secondary antibodies were added sequentially. Control tissues were prepared in a similar manner, omitting primary or secondary antibodies from the incubation solution. All primary antisera were diluted with 0.5% Triton X 100 (Sigma-Aldrich) in 0.01 M PBS (pH 7.2) to aid tissue penetration.

Tissues were examined using a Zeiss LSM 510 Meta confocal microscope (Carl Zeiss MicroImaging, Gottingen, Germany) with excitation wavelengths suitable for Alexa Fluor 488 or 594. Confocal micrographs of whole mounts were digital composites of the Z series of scans of 1-μm optical sections through the tissue depth. Images were constructed using Zeiss LSM 5 Image Examiner software and exported as TIFF files for final processing using Adobe Photoshop CS5 (Adobe Systems Inc., San Jose, CA) and Corel DRAW 7 software (Corel Inc., Mountain View, CA).

C. muridarum *infection*

The Weiss strain of *C. muridarum* was grown in HeLa 229 cells as previously described [18, 19]. Six- to seven-week-old BALB/c mice were treated with progesterone (DepoProvera, P4; Upjohn, Kalamazoo, MI) and were inoculated intravaginally 1 wk later with 100–200 median infective dose (5×10^3 to 10×10^3 infectious units) of *C. muridarum* (MoPn) [6]. Five to seven BALB/c mice were killed at each time point, 1, 2, 4, and 7 wk postinfection (8–15 wk old), and their oviducts were removed. One oviduct from each animal was reserved for electrophysiology and the remaining (contralateral) oviducts were used for immunohistochemistry. Age- and strain-matched mice were used as uninfected controls and received only the progesterone pretreatment.

Drugs and Solutions

The recording chamber was perfused at a rate of 3 ml min^{-1} with warmed oxygenated KRB of composition (in mmol/L): NaCl, 120.35; KCl, 5.9; NaHCO$_3$, 15.5; NaH$_2$PO$_4$, 1.2; MgCl$_2$, 1.2; CaCl$_2$, 2.5; and glucose, 11.5. 97% O$_2$-3% CO$_2$ was bubbled through the solution to maintain pH at 7.3–7.4 at 37°C $\pm$ 0.5°C. Prior to the commencement of recordings, oviducts were left to equilibrate in the recording chamber for 1 h. N$^\omega$-nitro-L-arginine (L-NNA) was purchased from Sigma-Aldrich and was dissolved in deionized H$_2$O to make a stock solution before being diluted in KRB and applied to oviducts to achieve the final desired concentration of 100 μM.

Statistical Analysis

Data are expressed as mean $\pm$ SEM, and n refers to the number of animals from which recordings were made. Intracellular recordings were analyzed using Clampfit 9.0 (Axon Instruments). Student *t*-tests were performed and the resultant *P* value was used to determine statistical significance. $P < 0.05$ was considered to represent a statistically significant change. Final figures were constructed from digitized data using Adobe Photoshop CS2 (Adobe) and Corel DRAW 7.

RESULTS

Time-dependent effects of *C. muridarum* infection on ICC-OVI and pacemaker activity were examined in oviducts taken from mice at times 0 (uninfected controls) and 1, 2, 4, and 7 wk after infection.

In uninfected oviducts resting membrane potential (RMP) averaged -59 ± 5 mV and spontaneous slow waves 37 ± 5 mV in amplitude with a half maximal duration of 1.6 ± 0.4 sec occurred at a frequency of 9.9 ± 0.8 cycles min^{-1}. The rate of rise of the upstroke of slow waves averaged 178 ± 5 mV sec^{-1} (n = 5; Fig. 1A). Immunohistochemistry with antibodies against KIT (ACK2), NOS2, and PTGS2 proteins was performed to assess expression in the ampulla, isthmus, and intramural segments of oviducts. In uninfected oviducts, KIT-immunopositive ICC-OVI anastomosing networks were found in all regions (Fig. 1, B–D). The distribution of ICC along the oviduct was similar to that previously reported (see Supplemental Fig. S2; Dixon et al. [9]). Occasional rounded NOS2-

FIG. 1. Pacemaker activity and expression of KIT, NOS2, and PTGS2 in uninfected control oviducts. **A**) An intracellular recording from an uninfected control oviduct revealing typical slow wave activity. **B–J**) Expression of KIT, NOS2, and PTGS2 in different segments of uninfected oviducts. KIT-immunopositive ICC-OVI networks (arrows) are found in the ampulla (**B**), isthmus (**C**), and intramural segments (**D**). **E–G**) Expression of NOS2 in few cells (arrows) in the similar segments. Small numbers of NOS2-positive cells were observed in the ampulla (**E**) and isthmus (**F**), whereas the intramural segment did not express NOS2 (**G**). **H–J**) The lack of PTGS2 expression in all oviduct segments. Bar in **J** = 50 μm and applies to all panels.
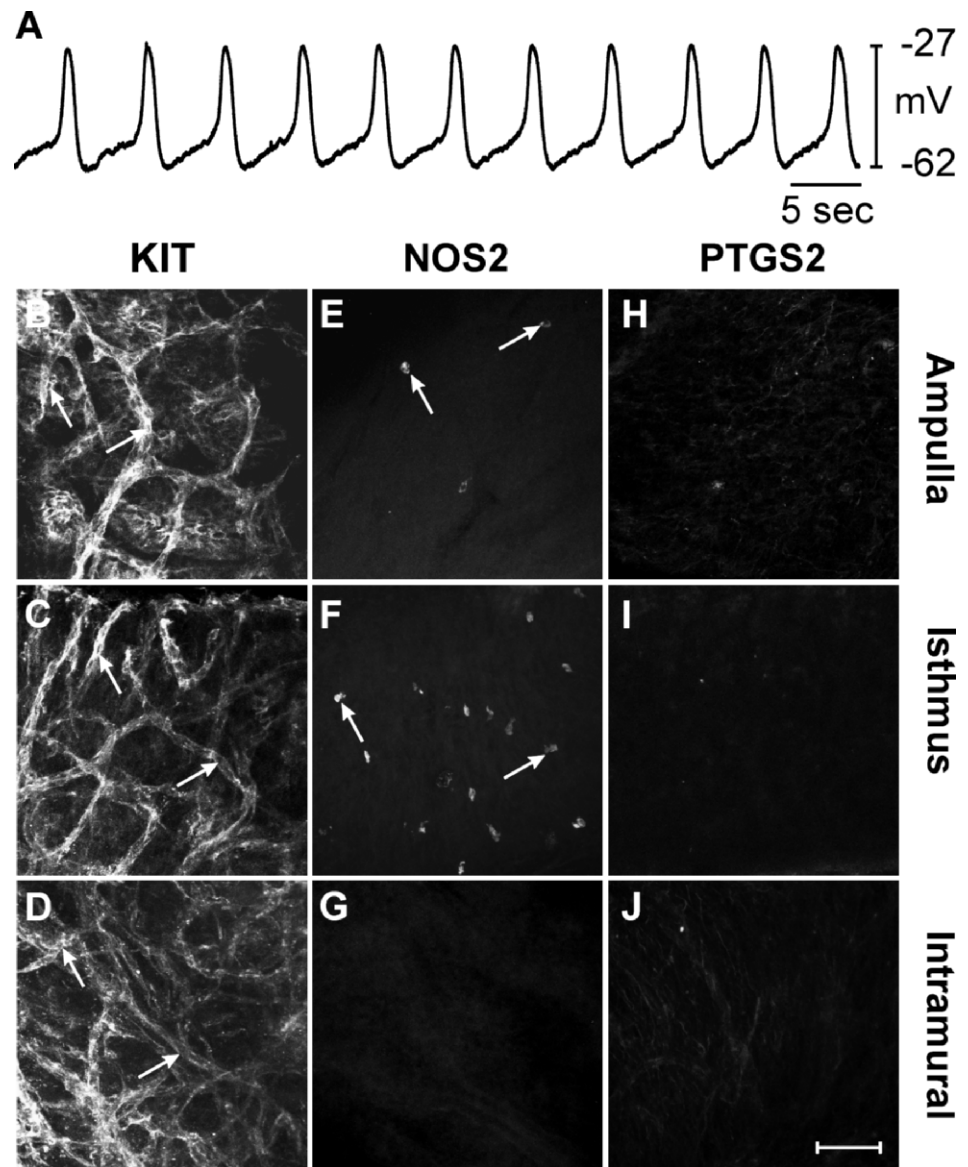
immunopositive cells were found in the ampulla and isthmic segments, but NOS2 immunoreactivity was not observed in intramural segments (Fig. 1, E–G). PTGS2-immunopositive cells were not observed in any segment of uninfected oviducts (Fig. 1, H–J).

One Week Postinfection

One week after *C. muridarum* infection, gross inspection revealed mild pyosalpinx and swelling in two of seven animals, which is typical for this strain [6]. Intracellular recordings were performed on oviducts of four animals that displayed no obvious sign of pyosalpinx and one that displayed mild pyosalpinx. RMP and slow wave activity were not statistically different from those of controls (n = 5; Fig. 2A). RMP averaged −59 ± 3 mV ($P = 0.992$, compared to uninfected control) and slow waves 36 ± 3 mV ($P = 0.916$) in amplitude with half maximal durations of 1.3 ± 0.3 sec ($P = 0.521$) occurred at a frequency of 9.5 ± 1 cycles min^{-1} ($P = 0.778$). The rate of rise of the upstroke of slow waves was also not significantly different, averaging 178 ± 13 mV sec^{-1} ($P = 1.000$). KIT immunohistochemistry revealed the presence of ICC-OVI in the ampulla, isthmus, and intramural segments of

mice 1 wk postinfection (Fig. 2, B–D). However, the ICC-OVI network appeared patchy and disrupted in the ampulla (Fig. 2B) but remained intact and comparable to the structure of ICC-OVI networks in the isthmus (Fig. 2C) and intramural segments in control mice (Fig. 2D). Because intracellular recordings were all performed at 50% along the length of oviducts, any change in pacemaker activity in the ampulla resulting from the disruption in the ICC-OVI network would not have been resolved. Immunohistochemistry of the ampulla segment revealed a marked increase in NOS2-positive cells that were often clustered together (Fig. 2E). These cells had a rounded morphology and were assumed to be leukocytes. In the more distal segments of the oviduct, NOS2-positive cells were much less dense, with only a few lone positive cells observed in the isthmus and intramural segments (Fig. 2, F and G). In contrast, PTGS2-positive cells were observed to be most dense in the intramural segment and gradually decreased so that the fewest cells were found in the ampulla (Fig. 2, H–J).

Two Weeks Postinfection

After 2 wk of infection all seven animals examined displayed bilateral pyosalpinx. The degree of pyosalpinx
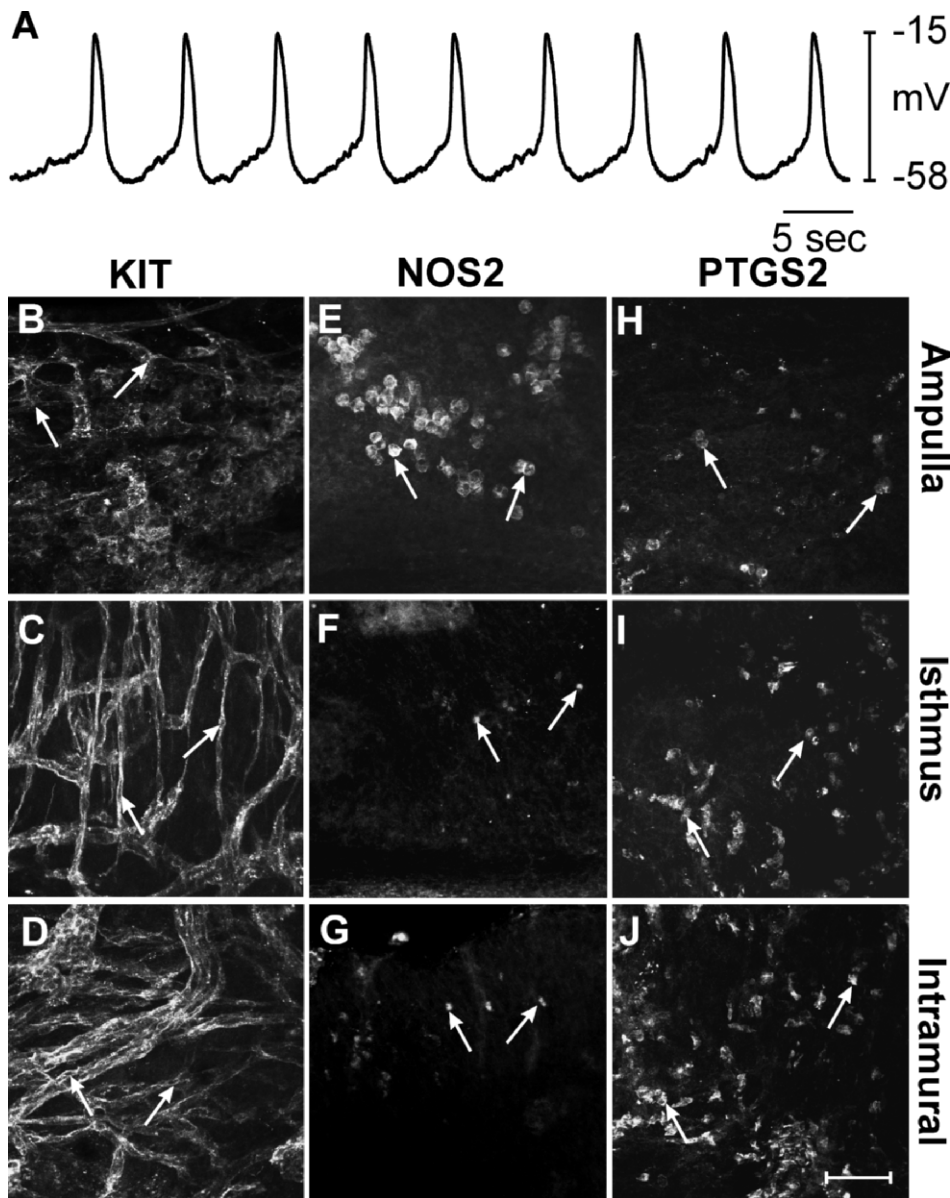
FIG. 2. Pacemaker activity and expression of KIT, NOS2, and PTGS2 in oviducts 1 wk after infection. **A–J**) Slow wave activity and expression of KIT, NOS2, and PTGS2 in oviducts 1 wk following infection with *C. muridarum*. **A**) An intracellular recording showing typical slow wave activity in the isthmus section of an oviduct 1 wk postinfection. **B–D**) The presence of KIT-immunopositive ICC-OVI along the length of an oviduct (arrows indicate cell bodies). The ICC-OVI network in the ampulla (**B**) appeared patchy and disrupted but remained intact in the isthmus (**C**) and intramural segments (**D**). **E–G**) Rounded NOS2-immunopositive leukocyte-like cells (arrows) along the length of an oviduct. A higher density of NOS2-positive cells was observed in the ampulla (**E**) compared to that seen in uninfected oviducts. Few NOS2-expressing cells populated the isthmus (**F**) and intramural segments (**G**). **H–J**) Increased numbers of PTGS2-positive cells (arrows) in the ampulla (**H**), isthmus (**I**), and intramural segments (**J**) of an oviduct 1 wk after infection. **H–J**) The lack of PTGS2 expression in cells of all oviduct segments. Bar in **J** = 50 μm and applies to all panels.

varied from mild to severe but all oviducts examined were swollen to some extent and contained inflammatory exudate. In 2 wk postinfection oviducts, RMP averaged -60 ± 7 mV ($P = 0.907$ compared to uninfected controls) and spontaneous slow waves were absent (n = 4; Fig. 3A). These findings are similar to previous results obtained from C3H/HeN mice at this time point [9]. The viability of the quiescent oviducts was examined using EFS. EFS (>3 ms) evoked myogenic depolarization responses (Fig. 3B), suggesting that the myosalpinx was viable and the loss of slow wave activity was not related to damage to smooth muscle cells. Immunohistochemical analysis with KIT antibodies revealed that ICC-OVI networks were absent from the ampulla (Fig. 3C). Small round isolated KIT-immunopositive cells with a morphology resembling mast cells [20] were present in the ampulla segment. ICC-OVI networks in the isthmus (Fig. 3D) and intramural segments (Fig. 3E) appeared patchy and disrupted compared to uninfected controls. This suggests that the lack of slow waves in oviducts after 2 wk of infection is a result of a damaged ICC-OVI pacemaker network. After 2 wk of infection, NOS2 immunoreactivity was observed in two different populations of cells. Rounded

NOS2-containing leukocyte-like cells were found within the pus-filled lumen of oviducts (data not shown) and stellate-shaped macrophage-like cells were found in the outer wall (the myosalpinx or serosa) of the ampulla (Fig. 3F), isthmus (Fig. 3G) and intramural segments (Fig. 3H). Double labeling using rat anti-mouse I-A^d/I-E^d and goat anti-mouse KIT monoclonal antibodies to recognize macrophages and ICC-OVI, respectively, revealed a close anatomical association between these cells within the uninfected oviduct (often <1 μm; Fig. 4). PTGS2-immunopositive cell populations were found to be greatest in the isthmus (Fig. 3J) and intramural segments (Fig. 3K) compared to the ampulla (Fig. 3I).

Four Weeks Postinfection

Four weeks after infection, pyosalpinx had resolved in all oviducts and was replaced by hydrosalpinx in three of five oviducts examined. At this stage intracellular recordings were made in five oviducts. In three of these oviducts (two of which had no obvious hydrosalpinx and one of which displayed mild hydrosalpinx), spontaneous slow wave activity

FIG. 3. Pacemaker activity and expression of KIT, NOS2, and PTGS2 in oviducts 2 wk after infection. **A–K**) Pacemaker activity and expression of KIT, NOS2, and PTGS2 in oviducts 2 wk after infection with *C. muridarum*. **A** and **B**) Intracellular recordings showing the absence of slow waves in oviducts. In **B,** EFS was used to excite the myosalpinx of infected oviducts (single pulses [1 p], 1–10-ms duration; delivered at arrows). Membrane depolarizations were evoked with pulse durations >3 ms showing that, although not spontaneously active, the myosalpinx is still excitable. **C–E**) KIT-immunopositive cells along the length of an oviduct. ICC-OVI were absent in the ampulla (**C**). The ICC-OVI network in the isthmus (**D**) and intramural segments (**E**) was disrupted and appeared patchy. Isolated KIT-positive mast cells (arrowheads) could be distinguished from ICC-OVI networks (arrows in **D** and **E**) based on their characteristic small, rounded morphology. **F–H**) NOS2-immunopositive cells (arrows) in the ampulla (**F**), isthmus (**G**), and intramural segments (**H**). These cells were identified as macrophage-like cells based on their stellate appearance. Rounded NOS2-expressing leukocyte-like cells were also observed in the pus-filled lumen of infected oviducts (data not shown). **I–K**) Rounded PTGS2-positive cells (arrows) in the ampulla (**I**), isthmus (**J**), and intramural segments (**K**). Bar in **H** = 50 μm (for **C–E** and **H**), bar in **K** = 50 μm (for **F** and **I–K**), and bar in **G** = 50 μm.
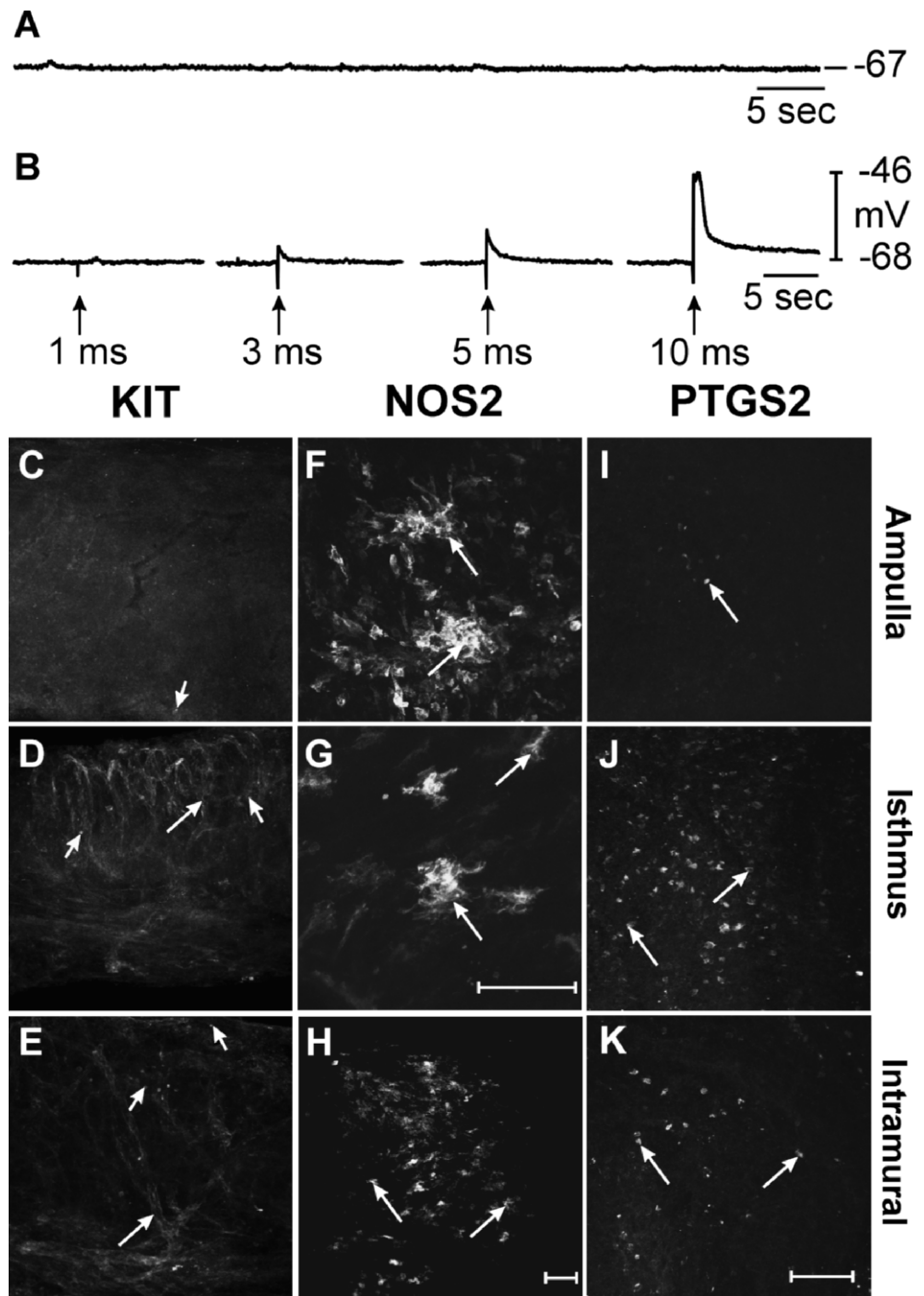
was present (Fig. 5A). RMP was slightly depolarized compared to uninfected controls, averaging -47 ± 6 mV, although this was not statistically significant ($P = 0.204$). Slow waves with an amplitude of 29 ± 3 mV ($P = 0.288$), a half maximal duration of 5.6 ± 0.2 sec ($P = 0.935$), and an upstroke rate of rise of 158.7 ± 12.2 mV sec^{-1} ($P = 0.127$) occurred at a frequency of 10.7 ± 0.4 cycles min^{-1} ($P = 0.519$). In the remaining two oviducts (both of which displayed marked hydrosalpinx), RMP averaged -71 ± 1 mV ($\sim$10 mV more hyperpolarized than uninfected controls) and slow wave activity was absent (Fig. 5, B and C). The myosalpinx of oviducts that lacked slow wave activity was still excitable as EFS (>3 ms) could evoke membrane depolarization (Fig. 5C). NO has been previously shown to have a potent relaxing effect on human Fallopian tubes [21,

22]. To determine whether endogenous NO production was inhibiting slow wave activity in the oviduct, we applied the NO synthase inhibitor L-NNA (100 μM). In the presence of L-NNA, RMP remained unaltered and slow waves did not return (data not shown). KIT immunohistochemistry revealed that some oviducts exhibited a complete lack of ICC-OVI along their entire length (Fig. 5, D–F), whereas others possessed ICC-OVI networks that appeared normal in the ampulla (Fig. 5G), isthmus (Fig. 5H), and intramural segments (Fig. 5I). This may explain why some oviducts did not display pacemaker activity whereas others displayed relatively normal activity. At this stage of the infection, NOS2-immunopositive macrophage-like cells were found in all segments of oviducts (Fig. 5, J–L) and an abundance of

PTGS2-positive cells was evident in all oviduct segments (Fig. 5, M–O).

Seven Weeks Postinfection

After 7 wk infection, two of five mice examined had bilateral hydrosalpinx, two had unilateral hydrosalpinx, and one had no obvious signs of hydrosalpinx. Three of the four oviducts on which intracellular recordings were performed displayed hydrosalpinx; however, slow waves were present in all oviducts (Fig. 6A). RMP averaged -58 ± 4 mV ($P = 0.942$) and slow waves with an amplitude of 36 ± 3 mV ($P = 0.882$) and half maximal duration of 2.5 ± 1.2 sec ($P = 0.474$), occurred at a frequency of 8.2 ± 2.2 cycles min^{-1} ($P = 0.441$). The upstroke phase of slow waves was significantly accelerated at 7 wk postinfection (215.7 ± 6.4 mV sec^{-1}) compared to that of controls (178.2 ± 4.9 mV sec^{-1}; $P = 0.002$). An extensive KIT-immunopositive ICC-OVI network, similar to uninfected controls, was evident along the length of oviducts after 7 wk of infection (Fig. 6, B–D). Very few NOS2-immunopositive macrophage-like cells were evident along the length of the entire oviduct (Fig. 6, E–G). PTGS2-immunopositive cells densely populated the intramural segment (Fig. 6J), but fewer numbers were found in the isthmus segment (Fig. 6I) and only occasional cells were present in the ampulla (Fig. 6H).

DISCUSSION

We have previously reported that ICC-OVI networks are disrupted 2 wk subsequent to *C. muridarum* infection and that this damage causes loss of spontaneous pacemaker activity and associated myosalpinx contractions, which are essential for egg transport through oviducts [9]. Two weeks of *C. muridarum* infection represents the peak of the oviduct involvement; however, the temporal relationship from onset to resolution of infection and disruption to ICC-OVI was not established in the previous study. In the present study we showed that ICC-OVI network disruption began in the ampulla segment of oviducts at 1 wk after infection. By 2 wk, the damage to the ICC-OVI networks had spread along the entire oviduct and associated spontaneous pacemaker activity was absent. At 4 wk, which is approximately the time when mice begin to resolve *C. muridarum* infection [4], ICC-OVI networks had recovered in 60% of oviducts examined and spontaneous pacemaker activity was resumed. In the remaining 40%, ICC-OVI networks were still absent and oviducts remained quiescent. By 7 wk, ICC-OVI networks were recovered in all segments and spontaneous pacemaker activity was restored in all oviducts.

At the peak of *Chlamydia* infection in mice it has been shown that loss of ICC-OVI and pacemaker activity is associated with an increase in NOS2 expression in oviducts [9]. It has also been shown that the inflammatory response caused by lipopolysaccharide leads to loss of spontaneous pacemaker activity and that this activity can be preserved and protected by adding the specific NOS2 inhibitor 1400W, providing evidence for the detrimental effects of NO production by NOS2 on oviduct pacemaker activity [9]. In the present study, the relative density of NOS2 and PTGS2-positive cells was monitored at specific time points after infection with *C. muridarum* to determine whether loss of spontaneous activity and damage to the pacemaking ICC-OVI networks correlated with an increase in inflammatory mediators. Disruption of ICC-OVI networks and loss of associated pacemaker activity occurred synchronously with a marked increase in NOS2-expressing cells early in the infection.
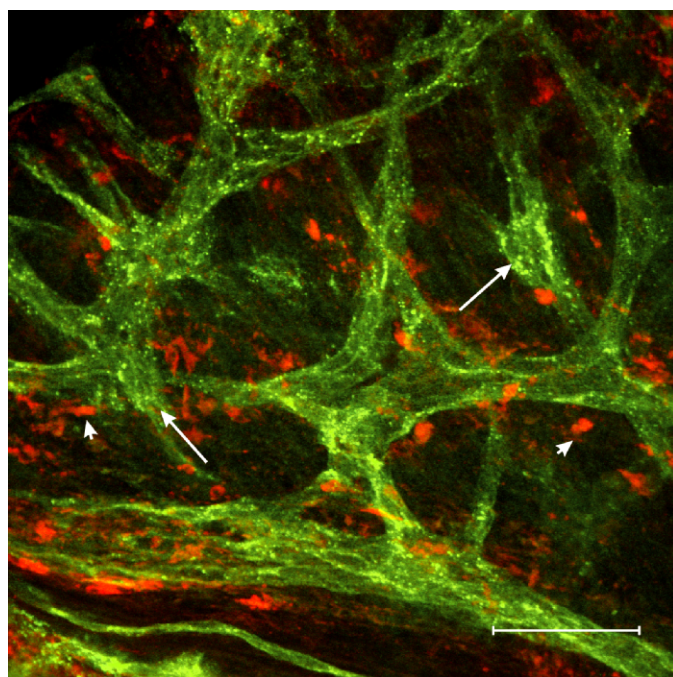

FIG. 4. KIT-positive ICC-OVI are located within close proximity to resident macrophages in uninfected oviducts. A confocal micrograph showing the close proximity of ICC-OVI (labeled using KIT and Alexa Fluor 488; green, arrows) and resident macrophages (labeled using I-A^d/I-E^d and Alexa Fluor 594; red, arrowheads) in an uninfected BALB/c oviduct. Note the anatomical relationship between ICC-OVI and macrophages is often <1 μm. Bar = 50 μm.

Interestingly, the ampulla segment appeared more sensitive to *Chlamydia* infection, with increased NOS2-positive cell expansion, disrupted ICC-OVI networks, and loss of pacemaker activity occurring before the isthmus segment showed signs of disruption. Why the ampulla segment is more sensitive to infection remains to be determined. Furthermore, upon resolution of the *C. muridarum* infection, which in mice typically occurs 3–4 wk postinfection [4], the density of NOS2-expressing cells declined, ICC-OVI networks recovered, and pacemaker activity resumed.

It has previously been established that NOS2 production is not essential for the resolution of *C. muridarum* infections. This is evidenced by the fact that $Nos2^{-/-}$ mice resolve *Chlamydia* infection within a similar time course as wild-type mice. The time course of infection was also reported to be similar when NOS2 was chemically inhibited with N^G-monomethyl-L-arginine (L-NMMA) in wild-type mice compared to controls [23–25]. Although NOS2 is not necessary for resolution of acute infection, $Nos2^{-/-}$ mice have been shown to display increased hydrosalpinx formation and infertility in response to *C. muridarum* infection [26], suggesting a role for NOS2 in protection from chronic *Chlamydia* disease [24]. In the present study we propose that a marked increase in NOS2 expression in macrophage-like cells is associated with disruption in ICC-OVI and decreased expression is associated with a recovery of ICC-OVI and pacemaker activity. However, the increased hydrosalpinx and infertility that occurs in $Nos2^{-/-}$ mice suggests that other factors may damage ICC-OVI or that there are compensatory roles in proinflammatory mediators in mice null for NOS2.

NOS2 and PTGS2 are inflammatory mediators that have been previously reported to have damaging effects on ICC of the gastrointestinal tract following abdominal surgery [27, 28].

FIG. 5. Pacemaker activity and expression of KIT, NOS2, and PTGS2 in oviducts 4 wk after infection. **A–O**) Pacemaker activity and expression of KIT, NOS2, and PTGS2 in oviducts 4 wk postinfection with *C. muridarum*. **A–C**) Intracellular recordings from infected oviducts. Spontaneous slow waves were observed in three out of five infected oviducts (**A**) but were absent in the remaining two oviducts (**B** and **C**). In **C**, EFS was used to excite the myosalpinx of an oviduct that did not display spontaneous activity (single pulses [1 p], 1–10-ms duration; delivered at arrows). Membrane depolarization of the myosalpinx occurred in response to EFS, suggesting that it was still excitable. **D–F** and **G–I**) KIT immunoreactivity along the length of two infected oviducts. ICC-OVI were absent along the entire length of the oviduct shown in **D–F**, whereas KIT-positive mast cells (arrowheads) could be recognized. In another oviduct, ICC-OVI (arrows) were arranged into networks and found in all segments, including the ampulla (**G**), isthmus (**H**), and intramural segments (**I**). Mast cells (arrowheads) were also found in the isthmus of the second oviduct (**H**). NOS2-positive macrophage-like cells (arrows) were present in each segment (**J–L**). The density of NOS2-positive macrophage-like cells was low in the ampulla (**J**) and higher in the isthmus and intramural segments (**L**). **M–O**) Dense populations of PTGS2-positive cells (arrows) in the ampulla (**M**), isthmus (**N**), and intramural segments (**O**). Bar in **I** = 50 µm (for **D–I**); bar in **L** = 50 µm (for **J–L**); bar in **O** = 50 µm (for **M–O**).
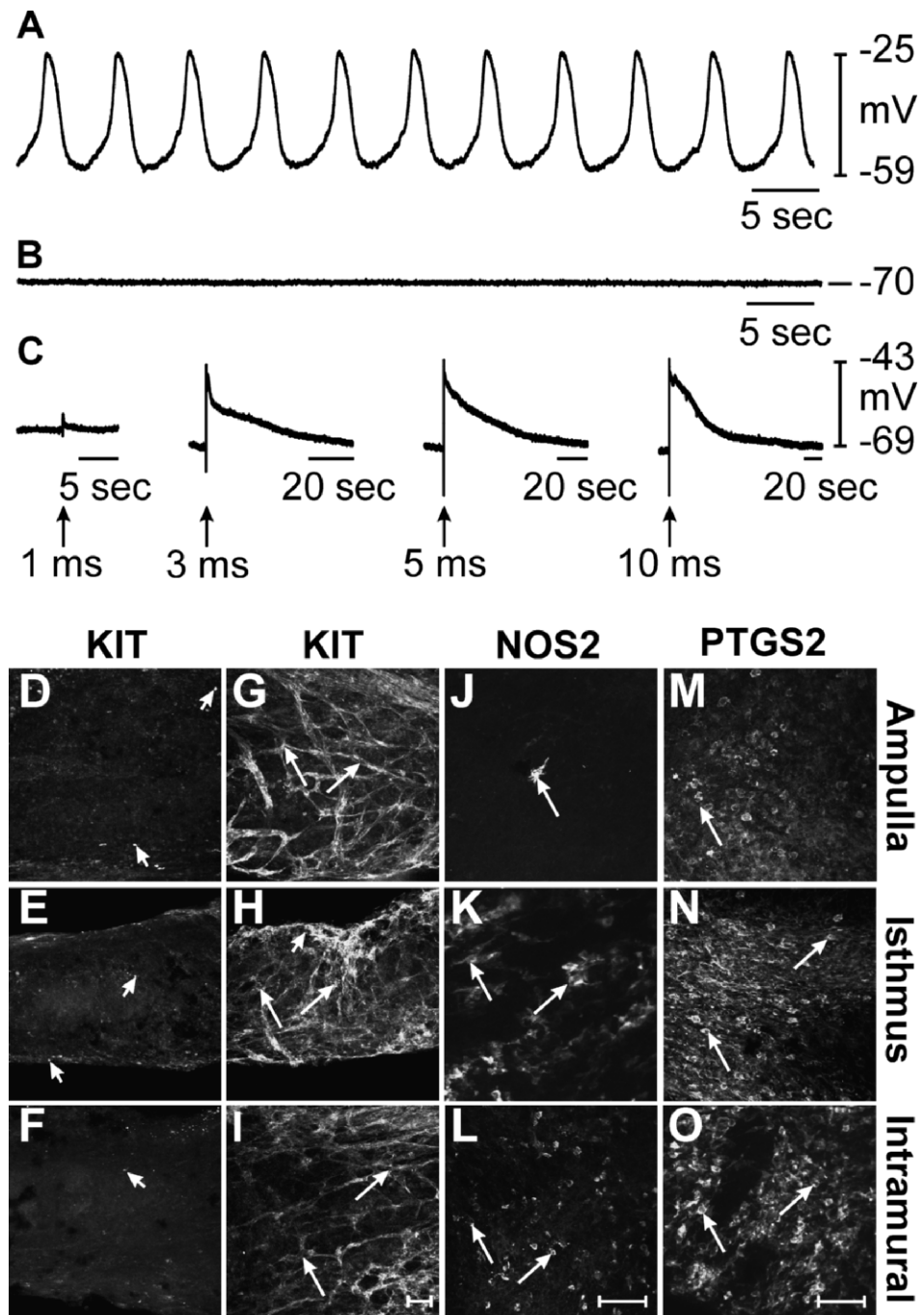
The resultant dysmotility of the GI tract occurs because of the loss of ICC and a subsequent reduction in slow wave activity, associated contractile activity, and postjunctional neural responses [27, 28]. The damaging role of increased expression of NOS2 and PTGS2 on ICC has been revealed in experiments in which $Nos2^{-/-}$ and $Ptgs2^{-/-}$ mice underwent intestinal resection and showed significant protection of ICC networks and pacemaker activity compared to controls that had undergone the same procedure [27, 28].

At 1 wk after infection. NOS2 appeared in rounded leukocyte-like cells, but by 2–7 wk postinfection, NOS2 expression appeared in stellate-shaped macrophage-like cells. Immunohistochemical analysis using macrophage markers on uninfected mice revealed that abundant numbers of resident macrophages exist within the oviduct wall and are anatomically

closely associated with ICC-OVI (Fig. 4). The close proximity between these two cell types suggests that a substance(s) produced by activated macrophages (i.e., NO) may affect ICC-OVI. Previous studies have demonstrated that inducible NOS (i.e., NOS2) is capable of prodigious production of NO, which may serve to elicit cell death or phenotypic changes in cells targeted by immune responses [29]. Elevated numbers of macrophages have been identified at sites distant to ectopic implantation sites in Fallopian tubes of women; these macrophages have been suggested to contribute to the embryo retention in the tube [30]. Increased expression of NOS2 in response to *Chlamydia* infection in humans has been linked to delayed tubal motility [31]. The elevation in macrophage-like cells and associated NOS2 expression observed in *Chlamydia*-infected oviducts in the present study may explain why women
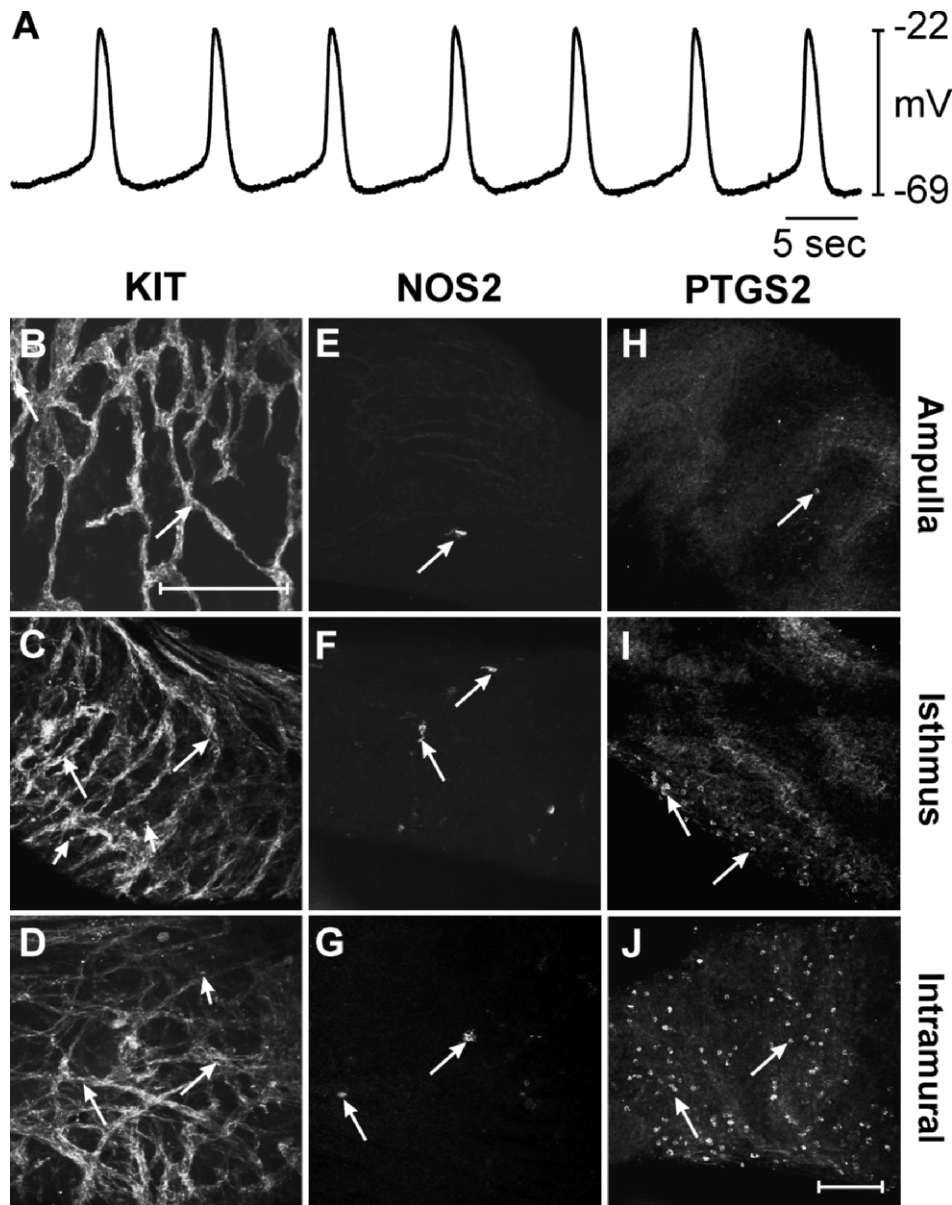
FIG. 6. Pacemaker activity and expression of KIT, NOS2, and PTGS2 in oviducts 7 wk after infection. **A–J**) Pacemaker activity and expression of KIT, NOS2, and PTGS2 in oviducts 7 wk postinfection with *C. muridarum*. **A**) An microelectrode recording showing spontaneous slow waves in an oviduct, 7 wk after infection. **B–D**) ICC-OVI networks in the ampulla (**B**), isthmus (**C**), and intramural segments (**D**). Arrows (**B–D**) indicate ICC-OVI; arrowheads (**C** and **D**) indicate mast cells. **E–G**) Low density populations of NOS2-positive macrophage-like cells (arrows) in the ampulla (**E**), isthmus (**F**), and intramural segments (**G**). **H–J**) PTGS2-positive cells (arrows) in the ampulla (**H**), isthmus (**I**), and intramural segments (**J**). Few PTGS2-positive cells were observed in the ampulla but populations were seen to gradually increase towards the distal end of the oviduct so that the intramural segment contained the greatest population of PTGS2-positive cells. Bar in **J** = 100 μm (for **C–J**) and bar in **B** = 100 μm.

with a history of multiple or chronic *Chlamydia* infections have increased risk for ectopic pregnancies.

The roles of prostaglandins (PGs) in the female reproductive tract (FRT) have been extensively reviewed. PGs that act on the oviduct originate from within the ovarian follicular cells, from the oviduct tubal fluid, and also from semen deposited in the FRT [32–35]. The concentrations of PGs along the oviduct vary depending on the segment. In the human ampulla, PGE_1 predominates, but in the isthmus, $PGF_{2\alpha}$ predominates [33]. In the oviduct myosalpinx, PGEs tend to be relaxant, whereas the PGFs tend to stimulate tubal contractility [32, 36]. The effect of PGs on a particular tissue is dependent upon the populations of PG receptor subtypes present in that tissue. PGEs act on E-prostanoid (EP) receptors, of which four subtypes have been identified, termed EP_1–EP_4 [37]. Agonist binding to EP_1 or EP_3 receptors in smooth muscle causes elevation of inositol 1,4,5-trisphosphate and increases intracellular Ca^{2+}, resulting in contraction, whereas binding to EP_2 or EP_4 leads to elevation of cAMP, resulting in relaxation [38]. PGFs act on stimulatory F-prostanoid receptors. The actions of PGE_1 on the myosalpinx differ in the two muscle layers of the human

oviduct [35, 39]. PGE_1 has been shown to stimulate the longitudinal muscle of the human Fallopian tube and relax the circular muscle [39], suggesting that different PG receptors may exist in the two muscle layers.

When induced in response to infection, PTGS2 leads to the production of PGs. The role of PTGS2 and associated PGs in the disruption of ICC-OVI is not clear. PTGS2-positive cells were not present in uninfected oviducts but began to appear along the length of oviducts 1 wk after infection. At 1 wk, the distribution of PTGS2-positive cells along the length of oviducts mirrored the ascending route of the *C. muridarum* infection, such that the highest density of PTGS2-positive cells was found in the intramural segment and gradually declined towards the ampulla. However, ICC-OVI networks appeared damaged at this time point in the ampulla but intact in the isthmus and intramural segments. Thus, there is a negative correlation between PTGS2-positive cell density and damage to ICC-OVI. After 4 wk of infection, PTGS2-positive cells were present at high numbers in all segments of the oviducts despite the resolution of infection and recovery of functional ICC-OVI networks. Finally, at 7 wk postinfection, when ICC-

OVI networks and associated pacemaker activity were fully recovered, PTGS2-positive cells were still quite abundant throughout the oviduct. These data suggest that increased PTGS2 is not directly involved in the inflammation-induced damage to ICC-OVI networks observed during *C. muridarum* infection, but may act as a compensatory agent stimulating smooth muscle contractions when ICC-OVI are damaged, although this would depend upon receptor profile expression in the myosalpinx during infection. It has been previously reported that PTGS2 expression is confined to epithelial cells in the female genital tract of *C. muridarum*-infected mice [40]. So it is possible that ICC-OVI lying within the myosalpinx simply are not exposed to the PTGS2 produced as a result of this infection. Future experiments should examine the effect of *C. muridarum* infection on ICC-OVI networks and pacemaker activity in *Nos2*$^{-/-}$ and *Ptgs2*$^{-/-}$ mice.

Although fertility was not assessed in the present study, *C. muridarum* infection of mice has been shown to cause infertility lasting beyond the period of infection [6]. Thus, the mice in our study were likely to have suffered compromised fertility or been rendered infertile [5, 6]. Our data show that functional ICC-OVI are reestablished within oviducts as *Chlamydia* infection resolves. Therefore, loss of pacemaker activity, per se, does not appear to explain sustained infertility as a result of *Chlamydia* infection [9]. Loss of ICC-OVI abolishes spontaneous contractions of the oviduct myosalpinx, producing a state of pseudo-obstruction and luminal stasis [9]. It is possible that the pyosalpinx, hydrosalpinx, and stasis associated with infection permanently damages excitation-contraction coupling in the oviduct, perhaps by promoting luminal scarring and/or fibrosis. Thus, it possible that even temporary loss of propulsive contractions might leave more permanent damage to the motor function of the oviduct, even after electrical pacemaker activity recovers. Future experiments to evaluate motor responses of the oviduct after infections will be required to test this hypothesis. It should be noted that the mouse model employed in these studies is more akin to acute chlamydial PID in humans. In humans rendered infertile by past *Chlamydia* infection, multiple or chronic infections are quite common and thereby elicit a persistent or recurring inflammatory response to the infection [41].

In summary, the present study shows the temporal relationship between increased NOS2 expression in leukocytes and macrophage-like cells and the loss of ICC-OVI and pacemaker activity in oviducts in response to the host inflammatory response to *C. muridarum* infection. After resolution of infection, cellular expression of NOS2 decreases and functional ICC-OVI networks recover. The acute loss of ICC-OVI associated with *Chlamydia* infection may initiate stasis and fibrosis, which might have long-lasting effects on the function of the oviduct.

REFERENCES

1. Centers for Disease Control and Prevention. Sexually Transmitted Disease Surveillance, 2008. Atlanta, GA: U.S. Department of Health and Human Services; 2009.
2. World Health Organization. Global Prevalence and Incidence of Selected Curable Sexually Transmitted Infections Overview and Estimates. Geneva, Switzerland: WHO; 2001.
3. World Health Organization. Global Strategy for the Prevention and Control of Sexually Transmitted Infections: 2006–2015: Breaking the Chain of Transmission. Geneva, Switzerland: WHO; 2007.
4. Brunham RC, Rey-Ladino J. Immunology of *Chlamydia* infection: implications for a *Chlamydia trachomatis* vaccine. Nat Rev Immunol 2005; 5:149–161.
5. de la Maza LM, Pal S, Khamesipour A, Peterson EM. Intravaginal inoculation of mice with the *Chlamydia trachomatis* mouse pneumonitis biovar results in infertility. Infect Immun 1994; 62:2094–2097.
6. Shah AA, Schripsema JH, Imtiaz MT, Sigar IM, Kasimos J, Matos PG, Inouye S, Ramsey KH. Histopathologic changes related to fibrotic oviduct occlusion after genital tract infection of mice with *Chlamydia muridarum*. Sex Transm Dis 2005; 32:49–56.
7. Read TD, Brunham RC, Shen C, Gill SR, Heidelberg JF, White O, Hickey EK, Peterson J, Utterback T, Berry K, Bass S, Linher K, et al. Genome sequences of *Chlamydia trachomatis* MoPn and *Chlamydia pneumoniae* AR39. Nucleic Acids Res 2000; 28:1397–1406.
8. Morrison RP, Caldwell HD. Immunity to murine chlamydial genital infection. Infect Immun 2002; 70:2741–2751.
9. Dixon RE, Hwang SJ, Hennig GW, Ramsey KH, Schripsema JH, Sanders KM, Ward SM. *Chlamydia* infection causes loss of pacemaker cells and inhibits oocyte transport in the mouse oviduct. Biol Reprod 2009; 80:665–673.
10. Talo A, Hodgson BJ. Electrical slow waves in oviductal smooth muscle of the guinea-pig, mouse and the immature baboon. Experientia 1978; 34:198–200.
11. Parkington HC. Intracellularly recorded electrical activity of smooth muscle of guinea pig oviduct. Am J Physiol 1983; 245:C357–C364.
12. Kishikawa T, Kuriyama H. Electrical and mechanical activities recorded from smooth muscle cells of the human fallopian tube. Jpn J Physiol 1981; 31:417–422.
13. Shafik A, Shafik AA, El SO, Shafik IA. Specialized pacemaking cells in the human Fallopian tube. Mol Hum Reprod 2005; 11:503–505.
14. Popescu LM, Ciontea SM, Cretoiu D, Hinescu ME, Radu E, Ionescu N, Ceausu M, Gherghiceanu M, Braga RI, Vasilescu F, Zagrean L, Ardeleanu C. Novel type of interstitial cell (Cajal-like) in human fallopian tube. J Cell Mol Med 2005; 9:479–523.
15. Popescu LM, Ciontea SM, Cretoiu D. Interstitial Cajal-like cells in human uterus and fallopian tube. Ann N Y Acad Sci 2007; 1101:139–165.
16. Torihashi S, Ward SM, Nishikawa S, Nishi K, Kobayashi S, Sanders KM. c-kit-dependent development of interstitial cells and electrical activity in the murine gastrointestinal tract. Cell Tissue Res 1995; 280:97–111.
17. Ward SM, Burns AJ, Torihashi S, Sanders KM. Mutation of the proto-oncogene c-kit blocks development of interstitial cells and electrical rhythmicity in murine intestine. J Physiol 1994; 480(pt 1):91–97.
18. Weiss E, Schramek S, Wilson NN, Newman LW. Deoxyribonucleic acid heterogeneity between human and murine strains of *Chlamydia trachomatis*. Infect Immun 1970; 2:24–28.
19. Caldwell HD, Kromhout J, Schachter J. Purification and partial characterization of the major outer membrane protein of *Chlamydia trachomatis*. Infect Immun 1981; 31:1161–1176.
20. Nissinen MJ, Panula P. Developmental patterns of histamine-like immunoreactivity in the mouse. J Histochem Cytochem 1995; 43:211–227.
21. Ekerhovd E, Brannstrom M, Alexandersson M, Norstrom A. Evidence for nitric oxide mediation of contractile activity in isolated strips of the human Fallopian tube. Hum Reprod 1997; 12:301–305.
22. Ekerhovd E, Brannstrom M, Weijdegard B, Norstrom A. Localization of nitric oxide synthase and effects of nitric oxide donors on the human Fallopian tube. Mol Hum Reprod 1999; 5:1040–1047.
23. Ramsey KH, Miranpuri GS, Poulsen CE, Marthakis NB, Braune LM, Byrne GI. Inducible nitric oxide synthase does not affect resolution of murine chlamydial genital tract infections or eradication of chlamydiae in primary murine cell culture. Infect Immun 1998; 66:835–838.
24. Ramsey KH, Miranpuri GS, Sigar IM, Ouellette S, Byrne GI. *Chlamydia trachomatis* persistence in the female mouse genital tract: inducible nitric oxide synthase and infection outcome. Infect Immun 2001; 69:5131–5137.
25. Perry LL, Feilzer K, Caldwell HD. Neither interleukin-6 nor inducible nitric oxide synthase is required for clearance of *Chlamydia trachomatis* from the murine genital tract epithelium. Infect Immun 1998; 66:1265–1269.
26. Igietseme JU, Perry LL, Ananaba GA, Uriri IM, Ojior OO, Kumar SN, Caldwell HD. Chlamydial infection in inducible nitric oxide synthase knockout mice. Infect Immun 1998; 66:1282–1286.
27. Yanagida H, Yanase H, Sanders KM, Ward SM. Intestinal surgical resection disrupts electrical rhythmicity, neural responses, and interstitial cell networks. Gastroenterology 2004; 127:1748–1759.
28. Yanagida H, Sanders KM, Ward SM. Inactivation of inducible nitric oxide synthase protects intestinal pacemaker cells from postoperative damage. J Physiol 2007; 582:755–765.
29. Coleman JW. Nitric oxide in immunity and inflammation. Int Immunopharmacol 2001; 1:1397–1406.

30. Tonello A, Poli G. Tubal ectopic pregnancy: macrophages under the microscope. Hum Reprod 2007; 22:2577–2584.
31. Refaat B, Al-Azemi M, Geary I, Eley A, Ledger W. Role of activins and inducible nitric oxide in the pathogenesis of ectopic pregnancy in patients with or without *Chlamydia trachomatis* infection. Clin Vaccine Immunol 2009; 16:1493–1503.
32. Goldberg VJ, Ramwell PW. Role of prostaglandins in reproduction. Physiol Rev 1975; 55:325–351.
33. Karim SM, Hillier K. Prostaglandins in the control of animal and human reproduction. Br Med Bull 1979; 35:173–180.
34. Lindblom B, Wilhelmsson L, Wikland M, Hamberger L, Wiqvist N. Prostaglandins and oviductal function. Acta Obstet Gynecol Scand Suppl 1983; 113:43–46.
35. Spilman CH, Harper MJ. Effects of prostaglandins on oviductal motility and egg transport. Gynecol Invest 1975; 6:186–205.
36. Spilman CH, Harper MJ. Effect of prostaglandins on oviduct motility in estrous rabbits. Biol Reprod 1973; 9:36–45.
37. Coleman RA, Smith WL, Narumiya S. International Union of Pharmacology classification of prostanoid receptors: properties, distribution, and structure of the receptors and their subtypes. Pharmacol Rev 1994; 46: 205–229.
38. Jabbour HN, Sales KJ. Prostaglandin receptor signalling and function in human endometrial pathology. Trends Endocrinol Metab 2004; 15:398–404.
39. Ingelman-Sundberg A, Sandberg F, Ryden G, Molfese A. The effect of prostaglandin E on the circular and longitudinal musculature of the human oviduct in vitro. Acta Obstet Gynecol Scand Suppl 1971; 9:51.
40. Liu W, Dubinett S, Patterson SL, Kelly KA. COX-2 inhibition affects growth rate of *Chlamydia muridarum* within epithelial cells. Microbes Infect 2006; 8:478–486.
41. Beatty WL, Byrne GI, Morrison RP. Repeated and persistent infection with *Chlamydia* and the development of chronic inflammation and disease. Trends Microbiol 1994; 2:94–98.